

A Data Mining Perspective of XRF Elemental Analysis from Pueblo People's Pottery

M. Castro-Colin^{1*}, E. Ramirez-Homs² and J. A. López²

¹*Bruker AXS GmbH, Karlsruhe-76131, Germany*

²*Department of Physics, El Paso, TX-79912, USA*

Email: m.castrocolin@gmail.com^{1*}; jorgelopez@utep.edu²

ARTICLE INFORMATION

Received: October 10, 2019

Accepted: January 20, 2020

Published online: February 28, 2020

Keywords:

X-ray fluorescence, Radiation, Spectrometry, Cluster Analysis, Data Mining, Archaeology, Provenance, Nondestructive testing analysis

ABSTRACT

Hierarchical clustering was used to identify elemental signatures in artifacts attributed to the Pueblo peoples. The artifacts in this study are pottery samples found at different sites in the state of New Mexico, USA. Three methods were applied: complete, average, and Ward. Their corresponding cophenetic correlation coefficients were used to contrast the three methods. Elemental characterization was only based on X-ray fluorescence excitation from a portable spectrometer with silver anode. The elemental correlations here disclosed by data mining techniques are expected to guide further archaeological studies and assist experts in the assessment of provenance and historical ethnographic studies.



DOI: [10.15415/jnp.2020.72016](https://doi.org/10.15415/jnp.2020.72016)

1. Introduction

Pottery, especially concerning ancient cultures, has an empirical basis which makes its study a complex task. Pottery achieves its characteristics through the manufacturing process, in addition to the raw materials that give it origin. It is perhaps one of the oldest incursions of early humans [2, 9] in the field of what is today called materials science. Pottery can provide a window into the geographical location of the makers, their technological advances, their trading practices, and even—without aforesought design—about the evolution of Earth's magnetic field [1].

Typically, provenance of archaeological artifacts is established by means of a well characterized sample—however, such a vantage point may not be always available to the researcher. The elemental composition and other physical and mineralogical as well as morphological factors are well known and compared against those of unknown artifacts [27]. In the case of pottery, the composition of clay beds is also compared to that of pottery samples [18], but clay is a complex material with ample geographical distributions and variations [22, 26]. An elemental composition match is a crucial factor in geographical provenance, but the lack of a match may not suffice to discard geographical provenance. To amplify the complexity of asserting provenance of pottery, details of firing temperature can alter both chemical

and mineralogical make up. Likewise, the addition of temper will affect chemically the clay [18].



Figure 1: Example of pottery samples used in the present study. There are no visible pigmented decorations and the surface may be visibly rough in some cases.

Determination of provenance consists not only of establishing geographical origin, but it extends to coordinates of time and ethnic origin. Information about the first two can be mostly gained from 1 multiple analytical techniques [2, 3, 9, 27], an example of which is X-ray fluorescence (XRF) analysis [4, 8, 15, 16].

The present study deals with pottery sherds (Figure 1) found at four different sites in New Mexico, USA. The localities are presumed to have been inhabited by the Pueblo peoples, but also by other ethnic groups [5, 6]. No other analytical techniques were employed and no sample(s) of determined provenance has been available to compare the findings of this study. This study is meant

to display preliminary results that will help to classify the multiple samples collected. At this time we have not intended to create an exhaustive treatment applying all clustering techniques but rather to create an exploratory guidance using statistical techniques.

2. Sample Description and Methods

A total of 12 samples from the Pueblo peoples were analyzed. The samples originate from four locations in New Mexico: Three Rivers, Mimbres, Chupadero, and an unknown location. Their average size is about 3.4 cm² and thicknesses of some 3 to 4 mm. They were not processed in any way. Eight of the samples were probed on the back and front, and the rest only studied on the front or back as indicated, Table 1.

Table 1: Twelve samples were analyzed, eight of them on the front and back, and the rest only on the front or back, as indicated by the sample name. The column, Ref. No., will be used to refer to the samples throughout the document to facilitate their treatment, in lieu of the sample name which was assigned during collection of the pottery samples. Measurements from the same samples are labeled with the same capital letter, following the sample number. The designation “back” corresponds to a visual inspection of sherd concavity.

Sample No.	Location	Sample name	Ref. No.
1	Three Rivers, red-on-terracotta	17153-Q_4852	19
		17153-Q_back_3126	18
2		17153-R_0438	17
		17153-R_back_4134	16
3		17153-S_4145	15
		17153-S_back_2238	14
4		17157-F_0232	13
		17157-F_back_4215	12
5	Unknown, redware	17153-A_1418	11
6		17153-B_back_5018	10
7		17153-C_5942	9
8		17297-D_3114	8
9		17297-D_back_1259	7
10		17297-E_back_0014	6
11	Mimbres, black-on-white	12363-H_1259	5
		12363-H_back_5339	4
12	Chupadero, black-on-white	15018-J_5056	3
		15018-J_back_0247	2
12		10532-O_1818	1
		10532-O_back_3549	0

We used a portable X-ray excitation source, XMET 300TX from Oxford Instruments. The anode material is Ag, and the operational parameters were 40 kV and 7 μ A for all samples. This instrument has an energy dispersive (EDX) detector of the SDD type and the spectra collected can be displayed using a 2048 multichannel analyzer (MCA) integrated in the portable X-ray source. For energy calibration we used the Ag K-alpha and the Fe K-alpha lines. The portable instrument was placed in close contact with the samples from which only conspicuous dust was removed before irradiating for 300 s each sample.

All spectra were analyzed by means of PyMCA, an open source, publicly available software developed at the European Radiation Facility [21]. Data reduction of the spectra yielded a collection of intensities that constitute a multidimensional elemental space-20 elements in total. The intensities were then processed through clustering analysis as well as principal component analysis (PCA). Data treatment was accomplished by scripts developed in Python: sorting of PyMCA data, clustering, and PCA.

3. Results and Discussion

Figure 1 shows the fluorescence spectrum corresponding to sample 0 (10532-O_back_3549). The spectrum is shown in logarithmic scale to highlight the quality of the fit. A blue line (continuous line) represents the raw spectrum, the continuum background is colored gray (vertical line), and the fit is the green line (cross). The Compton portion of the spectrum is not included in the fit but it is inconsequential to the analysis since all elemental peaks included in the fit are well outside the Compton region at about 21 keV. All fits were of the similar quality but they are not included in the manuscript.

The most prominent spectral contribution is that of iron. High concentrations of iron are not uncommon in pottery artifacts [1, 24, 25]. The presence of Fe may be structural, since Fe acts substitutionally for major elements like Al or Mg, but it could also be present when added as temper or in the form of a pigment [24].

Elemental fits of the spectra were organized for analysis (Supplementary material Tables S2–S4). The values are the integrated counts per 300 s. A scree plot of the eigenvalues of PCA helped us identify the number of factors that we could retain to describe data dispersion. It would thus appear that two principal components would describe the overall data tendencies (Figure 2). Figure 2 was created after removing the elemental column corresponding to Fe. We have done that to better observe the elemental compositions that could guide classification of the samples: Sr, Zr, Ca, and Rb. Elemental concentrations have not been calibrated but that event is not relevant to the present treatment because

a correspondence between counts and concentrations can always be established. The table constitutes the elemental data matrix processed by hierarchical clustering techniques as well as PCA. In the hierarchical clustering analysis-the main technique employed-three methods were applied: complete, average, and Ward. In each case the same distance matrix was used as data precursor.

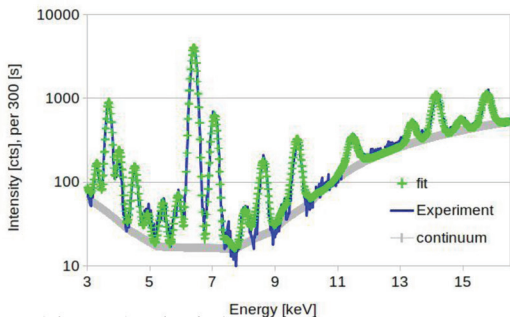


Figure 2: Raw spectrum (blue line), continuum (gray with vertical line), and elemental fit (green cross) from sample 10532-O_back_3549. A logarithmic scale is used to highlight the quality of the fit.

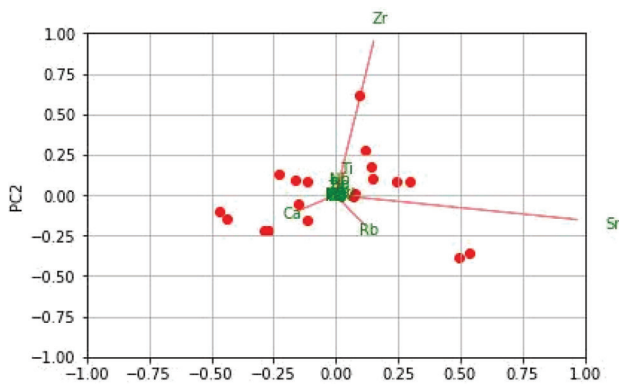
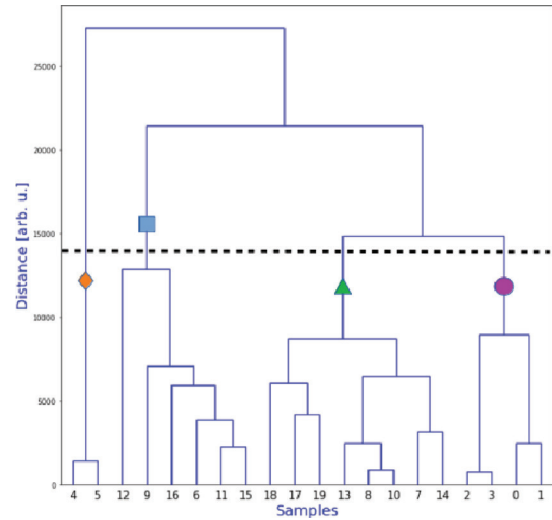


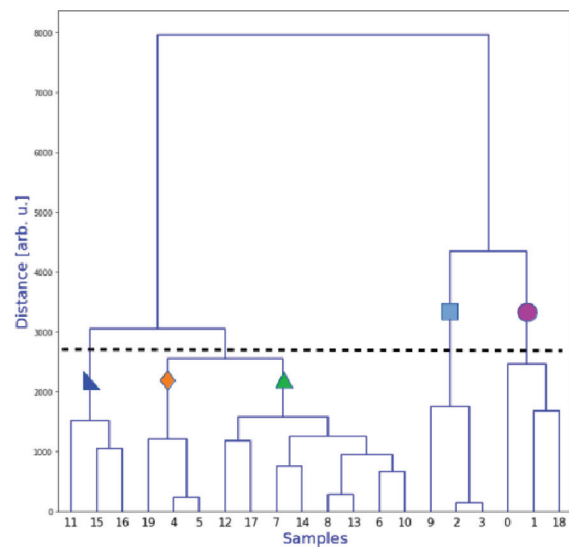
Figure 3: PCA was used to identify the main elemental components that describe the data matrix. The biplot was constructed after projecting the data on the plane of the two principal components. Intensities corresponding to Fe were removed prior to PCA analysis.

We are interested in finding correlations among the samples based, at this time, solely on their elemental signatures. Clustering analysis [12, 15, 23] is a convenient approach to extracting correlations out of seemingly disconnected data. The data is simultaneously expected to exhibit a connectivity pattern that would arise from a metric and a clustering method introduced to sort the data. At the outset, and for the sake of being systematic, the same Euclidean metric was used to construct the data matrix which subsequently was clustered by three other methods.

Supplementary Tables S2–S4 served to classify the samples as a function of their elemental composition.



(a)



(b)

Figure 4: Complete-linkage method dendrograms applied to the entire elemental content (a) and to clay elemental content. (b) Symbols are placed to aid the eye and the dashed line is the cut point.

Details of the manufacturing protocol of the pottery samples are unknown. With that idea in mind we decided to not only analyze the whole elemental composition of the sample, but to additionally create two elemental subgroups: clay and complementary. Thus we artificially created three data sets. In an initial step all elements identified were processed together. Subsequently generic elements typically

found in clay [14, 22] were processed alone: Fe, Ca, K, Ti, Cu, Mn, and Zn. The rest of elements, here called complementary, were also processed as an independent data set. The latter could be considered to have been added by their manufacturing process, perhaps temper, glazing or pigments, and/or through weatherizing throughout time and possibly handling.

Dendrograms are used to depict clustering. The hierarchical clustering algorithm proceeds by merging smaller clusters into larger ones and also splitting them, based on a distance criterion. In our case the factors are distances between vectors of elemental content. The samples have no visible decorations on them and pigmentation of that nature could not be gauged unequivocally (Figure 1). We included symbols in all figures corresponding to dendrograms. They facilitate identification of groups with the dashed line establishing a grouping boundary.

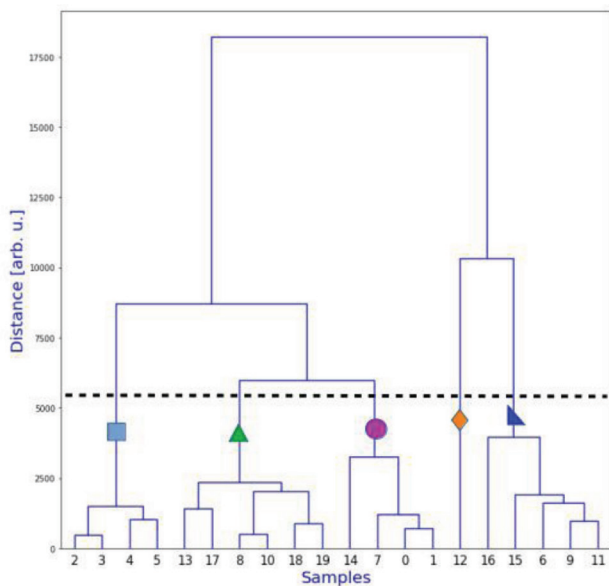
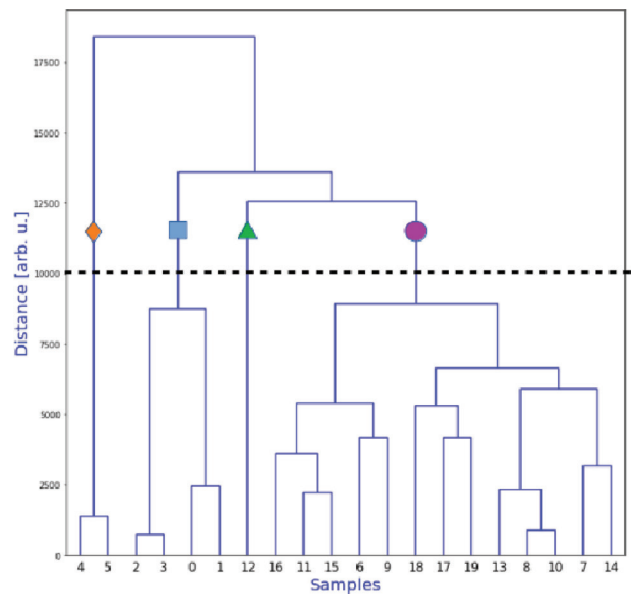
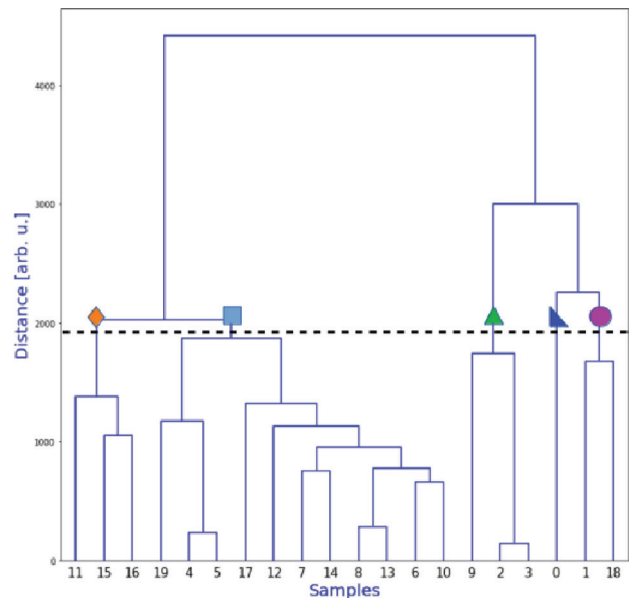


Figure 5: Complete-linkage method dendrogram of the complementary-element data set.

Complete-linkage method yielded the dendrograms in Figure 4. The entire data set was clustered into four well defined groups (Figure 4a). Clay elemental composition clustered the samples into five groups (Figure 4b). Complementary elements were also clustered into five groups (Figure 5). The average-linkage method applied to the entire data set yielded four groups (Figure 6a) and that applied to elemental clay yielded five groups (Figure 6b). The analysis of the complementary-element data set clustered the samples into five groups (Figure 7). The dendrograms generated using the third method, Ward, based on all elements, the clay elemental content, and the complementary-element set are given in Figures 8a, 8b, and 9, respectively.



(a)



(b)

Figure 6: Average-linkage method dendrograms applied to the entire elemental content (a) and to clay elemental content (b).

Each clustering method was designed with some classification capability in mind [13]. However, the adequacy of the method is commensurate to the geometrical distribution of the data and the type of information sought. Possibly, if the data has a two-dimensional representation, a clustering method may be readily selected, but that is not so in the present case. Let us highlight once again that we are only searching for a statistically educated sense of perspective to guide future research decisions.

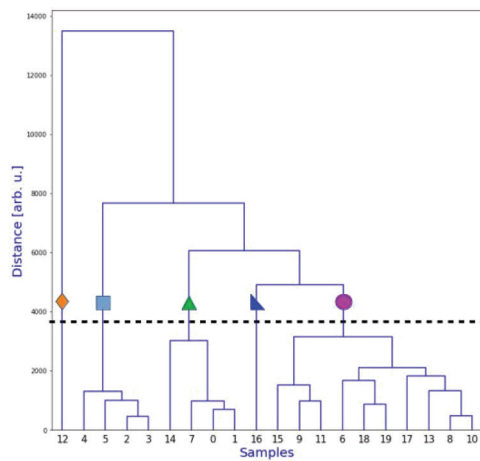
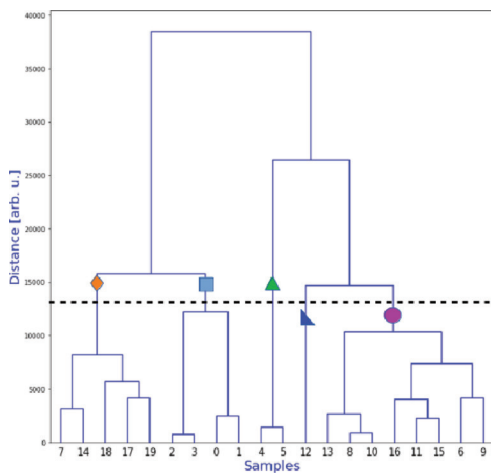
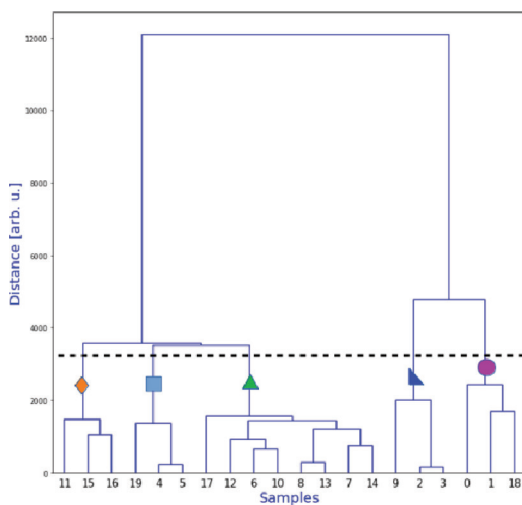


Figure 7: Average-linkage method dendrogram obtained from the complementary-element data set.



(a)



(b)

Figure 8: Ward metric dendrograms applied to all elements (a) and to clay elemental content (b).

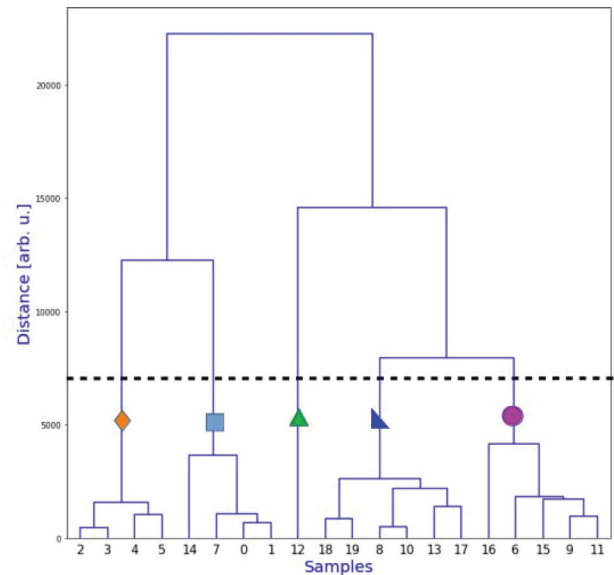


Figure 9: Ward metric dendrogram generated from only complementary elemental content.

An objective method was applied to quantify the degree of faithfulness of the pairwise distances that resulted from the clustering process in respect to the initial data matrix. Thus a cophenetic correlation coefficient [7, 20] was calculated for each data set and clustering methodology (Table 2). It serves as a qualification that helps us reduce the possibility of focusing on random effects driven intrinsically by the methodology itself.

Table 2: Cophenetic correlation coefficients from each data set and clustering methodology. The coefficients are closer to one for the average-linkage method.

Clustering method	All elemental data	Clay elemental data	Compl. elemental data
Complete	0.74042	0.80282	0.55909
Average	0.81454	0.80642	0.88105
Ward	0.63465	0.79599	0.65715

4. Summary

Pottery sherds were collected from three known locations in New Mexico and exposed to Ag X-ray radiation to extract elemental signatures from fluorescent excitation. Subsequently, elemental data were organized into a matrix where each sample has elemental variables that were hierarchically clustered using three methods. We did not mean to impose the use of any particular method or to preselect certain sample groups or numbers of groups during the treatment. For that reason we employed hierarchical

clustering methods that have relatively simple algorithms. The application of multivariate data mining methods, clustering, and PCA has been of a merely exploratory nature to numerically select elemental signatures for further investigation. Also, we have sought to assist reclassification of some of the samples. Both objectives have been aided by the numerical perspective provided by clustering methods.

Front and back of most samples were analyzed, with the dual intent of enhancing the objectivity of clustering and exploring whether clustering could be indicative of the manufacturing process of pottery making. Depending on the manufacturing process the elemental concentrations of front and back would be closely related. However that need not be the case, because the manufacturing process is not known and need not be the same on both sides of the sherd. Additionally, other factors, such as pigmentation, could create a factor of elemental discrepancy. Decorative pigmentation is not visually conspicuous on the samples here analyzed, however.

A favorable correspondence was found between the cophenetic correlation coefficient and features already known about the samples, which were highlighted by the average-linkage method. The average-linkage method, which has the highest cophenetic correlation coefficient, reflects the best correspondence with the geographical location known-data element 12 would have to be set aside. Such a conclusion is suggested only by the complementary elemental composition (Figure 7). The same dendrogram would also suggest a reclassification of samples 6 to 11, which are of unknown geographical origin. Notice that this vantage point only arose after splitting of the data set into two: clay and complementary elemental components. We are aware that the validity of the cophenetic correlation coefficient has been questioned [7, 17, 19]. Nevertheless, we used it because it is frequently applied in data mining techniques and clustering applications and it is of simple implementation.

As it has already been noted, average-linkage does not match front and back of each sample, which is of no concern. All clustering methods here applied yielded the same generic conclusion of front and back elemental mismatch. Invariably, all clustering methods paired together the front and back of samples (0,1), (2, 3), and (4, 5). It may be inferred that there are peculiarities about their manufacturing process, and detailed analytical investigations by other techniques should follow.

As suggested by the PCA results and to narrow down the scope of analysis and focus the analytical efforts, Fe, Sr, Zr, Ca, and Rb should be analyzed in future studies of the same samples. Kuleff and Djingova [10] have listed the former elements among the most important 23 elements in determining provenance of pottery. Future studies should also extend the elemental range of characterization below the

K K-alpha line, which was not possible with the excitation source available at present. Elemental content and its depth distribution will be investigated by X-ray photoelectron spectroscopy and will also be cluster-analyzed on its own to compare with the present findings. In the future we will also collect X-ray diffraction data, which is expected to shed more light about the elemental variations of Fe, Sr, Zr, Ca, and Rb identified by PCA.

Acknowledgments

We would like to acknowledge Dr. Charmichael (UTEP) for providing the samples and the technical support of the students of the MASE class at UTEP supervised by one of the authors, JAL. The views and opinions in this article are those of the author(s) and do not necessarily reflect the views and opinions of Bruker AXS or any of its affiliates.

References

- [1] E. Ben-Yosef, et al., PNAS **114**, 2160 (2009). <https://doi.org/10.1073/pnas.1615797114>
- [2] E. Boaretto, et al., PNAS **16**, 9595 (2017). <https://doi.org/10.1073/pnas.0900539106>
- [3] G. Bronitsky., Adv. Archaeological Method and Theory **9**, 209 (1986). <https://doi.org/10.1016/B978-0-12-003109-2.50008-8>
- [4] A. Chudin, K. Ushanova, and E. Lähderanta., Mediterranean Archaeology and Archaeometry **19**, 25 (2019). <https://doi.org/10.5281/zenodo.2585948>
- [5] J. Diamond. Collapse: how societies choose to fail or succeed. Ch. 4. pp. 145. Penguin Group, New York, USA (2005).
- [6] B. P. Dutton. "American Indians of the Southwest". Ch. 2, pp. 9-62. U. of New Mexico Press, Albuquerque, USA (1983).
- [7] M. Holgersson., Pattern recognition **10**, 287 (1978). [https://doi.org/10.1016/0031-3203\(78\)90038-9](https://doi.org/10.1016/0031-3203(78)90038-9)
- [8] A. Iordanidis, J. Garcia-Guinea and G. Karamitrou-Mentessidi., Mat. Characterization **60**, 292 (2009). <https://doi.org/10.1016/j.matchar.2008.08.001>
- [9] Y. Konomata, et al., Antiquity **93**, 1 (2019). <https://doi.org/10.15184/aqy.2019.56>
- [10] I. Kuleff and R. Djingova., Revue d'Archéométrie **20**, 57 (1996).
- [12] I. Liritzis, N. Zacharias, I. Papageorgiou, A. Tsaroucha and E. Palamar., Studia Antiqua et Archaeologica **24**, 31 (2018).

- [13] F. Murtagh and P. Contreras., Wiley Interdisciplinary Reviews: Data Mining and Knowledge Discovery **2**, 86 (2012). <https://doi.org/10.1002/widm.53>
- [14] P. S. Nayak and B. K. Singh, Bull. Mater. Sci. **30**, 235 (2007). <https://doi.org/10.1007/s12034-007-0042-5>
- [15] R. Norstrom, Graduate Thesis and Dissertations, U. of South Florida, January 2014
<http://scholarcommons.usf.edu/etd/5285>.
- [16] C. Papachristodoulou, et al., Anal. Chimica Acta **573**, 347 (2006).
<https://doi.org/10.1016/j.aca.2006.02.012>
- [17] J. B. Phipps, Systematic Zoology **20**, 306 (1971).
<https://doi.org/10.2307/2412343>
- [18] P. M. Rice and M. E. Saffer, J. Arc. Sci. **9**, 395 (1982).
[https://doi.org/10.1016/0305-4403\(82\)90045-0](https://doi.org/10.1016/0305-4403(82)90045-0)
- [19] F. J. Rohlf and D. L. Fisher, Systematic Zoology **17**, 407 (1968). <https://doi.org/10.1093/sysbio/17.4.407>
- [20] R. R. Sokal and S. J. Rohlf, Taxon **11**, 33 (1962).
<https://doi.org/10.2307/1217208>
- [21] V. A. Solé, E. Papillon, M. Cotte, Ph. Walter and J. Susini, Spectrochim. Acta Part B **62**, 63 (2007).
<https://doi.org/10.1016/j.sab.2006.12.002>
- [22] A. Sturz, M. Itoh, and S. Smith, Proceedings of the Ocean Drilling Program, Scientific Results **158**, 277 (1998).
<https://doi.org/10.2973/odp.proc.sr.158.221.1998>
- [23] R. H. Tykot, Appl. Spectroscopy **70**, 42 (2015).
<https://doi.org/10.1177/0003702815616745>
- [24] U. Wagner, et al., Radiation in Art and Archaeometry, Eds. D. C. Creagh and D. A Bradley. Ch. 18, 417-443. Elsevier Science, Amsterdam, The Netherlands (2000).
- [25] S. Watanabe, et al., Spec. Acta Part A: Mol. and Biomol. Spectroscopy **71**, 1261 (2008).
<https://doi.org/10.1016/j.saa.2008.03.034>.
- [26] J. B. Weems (1903). Chemistry of Clays. Iowa Geological Survey Annual Report, 14, 319-346.
- [27] A. L. Wilson, J. Archaeological Sci. **5**, 219 (1978).
[https://doi.org/10.1016/0305-4403\(78\)90041-9](https://doi.org/10.1016/0305-4403(78)90041-9)

Supplementary Material

Table S1: The elemental concentrations corresponding to each sample are organized in three tables only for the sake of visual convenience. This table presents elements from Fe to Ti.

Sample name	Element Ref. No.	Fe 0	Ca 1	K 2	Sr 3	Au 4	Ti 5
10532-O_back_3549	0	52200.7845	9641.6906	1366.3977	13868.2406	7660.0901	1431.0032
10532-O_1818	1	51448.5559	7591.8469	1272.4905	12730.7545	7505.3162	1440.3332
15018-J_back_0247	2	77377.7192	5603.1463	1947.7371	16932.352	9343.3797	1596.9853
15018-J_5056	3	81827.9634	5568.882	1899.6266	16377.4913	9297.1808	1525.7864
12363-H_back_5339	4	97302.7593	3269.4203	2300.1172	37859.1593	8511.1228	1552.8476
12363-H_1259	5	94770.186	3452.0633	2269.0996	38776.1962	8800.5061	1421.3949
17297-E_back_0014	6	167946.656	2765.972	2139.1901	30073.8091	8420.0741	3309.6646
17297-D_back_1259	7	118928.4879	2321.9132	1532.9238	21484.8811	7511.1629	2467.693
17297-D_3114	8	157314.5452	3090.8682	1600.1467	25899.2347	8233.2464	2622.2366
17153-C_5942	9	151337.8328	6167.0862	2103.054	31828.9815	9530.5911	3022.5433
17153-B_back_5018	10	144872.7207	2587.2749	1685.7353	25919.0465	8028.9217	3066.9293
17153-A_1418	11	285571.2316	3020.5177	2421.8834	26995.5792	8910.1604	4006.21
17157-F_back_4215	12	83393.6032	2555.3197	1653.8712	24228.9976	8678.3639	3705.237
17157-F_0232	13	223018.2954	2889.2337	1745.4456	24052.443	8685.3318	2626.4125
17153-S_back_2238	14	103226.4312	2353.5997	1424.6744	19969.2038	8258.8175	2822.7115
17153-S_4145	15	125061.7706	3551.6134	1990.3292	27254.154	9707.2647	3496.9418
17153-R_back_4134	16	120799.9956	4040.1039	2461.103	25996.5192	9050.0421	3047.9677
17153-R_0438	17	123427.4706	1962.3671	1570.5754	20263.4626	8672.6592	3083.3917
17153-Q_back_3126	18	88566.994	7749.0878	1797.1201	19990.8025	8332.9874	2464.8193
17153-Q_4852	19	82291.3545	4009.0998	1758.3169	17620.6683	7953.5071	2115.4966

Table S2: The elemental concentrations corresponding to each sample are organized in three tables only for the sake of visual convenience. This table presents elements from Rb to Cr.

Sample name	Element Ref. No.	Rb 6	Pd 7	Hg 8	Cu 9	Ni 10	Ga 11	Cr 12
10532-O_back_3549	0	3379.7417	164.8697	275.51	447.0367	86.2716	180.3862	493.62
10532-O_1818	1	2928.0506	148.4017	139.8503	415.3822	107.5726	98.7682	424.3268
15018-J_back_0247	2	9951.4367	20.3069	120.8616	355.0725	75.6996	290.4848	384.8009
15018-J_5056	3	10061.0292	255.4909	12.7576	328.2677	122.0444	282.5887	412.2964
12363-H_back_5339	4	9183.7742	5.9593	48.5688	370.4854	133.2249	166.7839	536.1078
12363-H_1259	5	9541.8167	58.8653	216.6187	397.6146	64.8448	146.264	518.7136
17297-E_back_0014	6	5547.3726	20.6025	373.7751	479.6883	148.059	250.0147	595.9227
17297-D_back_1259	7	3759.2627	120.2392	431.567	349.325	41.2896	185.3457	419.2235
17297-D_3114	8	4549.8689	178.278	304.8244	386.138	29.2074	248.6858	548.4017
17153-C_5942	9	5761.6696	153.6697	489.743	318.5314	32.8587	285.6738	633.5601
17153-B_back_5018	10	4305.2993	10.1688	405.074	314.4527	72.298	167.1197	550.404
17153-A_1418	11	5778.6575	248.2855	482.4386	378.1096	157.1728	187.2848	844.9983
17157-F_back_4215	12	5759.8177	56.0794	4.3725	362.776	52.5504	254.9801	472.1334
17157-F_0232	13	5544.4697	223.9691	545.4828	281.9956	2.9587	183.0174	706.9288
17153-S_back_2238	14	5190.9129	26.0582	315.6169	514.9722	146.9134	329.7659	512.5125
17153-S_4145	15	6504.2911	60.6155	244.6947	480.4863	153.389	457.7708	548.3078
17153-R_back_4134	16	6305.176	13.1743	280.8815	326.2293	32.1506	189.5267	496.2766
17153-R_0438	17	5648.5528	9.2811	463.555	381.8265	77.7758	299.7449	521.6246
17153-Q_back_3126	18	4519.0923	130.9969	82.1517	402.4156	69.2816	224.6812	442.793
17153-Q_4852	19	4248.848	32.2007	80.3864	445.1566	75.4794	143.4295	561.9875

Table S3: The elemental concentrations corresponding to each sample are organized in three tables, only for the sake of visual convenience. This table presents elements from Pb to Nb.

Sample name	Element Ref. No.	Pb 13	Mn 14	Y 15	Zn 16	Zr 17	Nb 18	Ag 19
10532-O_back_3549	0	367.7916	622.5391	2264.9483	2095.6551	10970.1327	90.0603	37.8725
10532-O_1818	1	385.118	621.7936	1973.7508	1928.3192	11322.225	117.3533	11.7112
15018-J_back_0247	2	967.951	2070.9733	3060.4677	2432.6328	10513.1978	660.1271	5.5716
15018-J_5056	3	946.0033	1968.1192	2832.663	2402.1609	10501.3086	420.9841	136.0308
12363-H_back_5339	4	671.4353	1009.5113	2619.9632	2281.0055	10053.5512	9.6727	93.0413
12363-H_1259	5	723.8238	1038.5169	2703.3912	2302.4663	10919.6033	200.3692	167.7075
17297-E_back_0014	6	1173.0341	1348.4712	2730.6879	2136.1045	17603.0002	932.799	191.7161
17297-D_back_1259	7	883.7682	825.7425	2428.8803	2001.4006	11018.1032	382.0076	12.6967
17297-D_3114	8	853.7281	1277.1264	2641.5996	2107.7728	14989.947	881.7279	54.0419
17153-C_5942	9	1467.3757	1373.0712	3517.1833	2094.2434	18334.0789	916.875	339.6938
17153-B_back_5018	10	1049.3692	1011.2292	2547.1445	2137.8239	15170.3263	805.9158	43.3431
17153-A_1418	11	1425.4369	1884.1235	3132.8347	3616.2393	18864.9045	1029.7486	484.3244
17157-F_back_4215	12	1313.3899	854.8612	2701.0743	2579.4799	27845.7102	1692.6629	383.2328

17157-F_0232	13	1161.7098	1246.8282	2511.239	2025.2887	15145.2998	765.6966	16.4449
17153-S_back_2238	14	1403.566	808.6286	2528.9161	2630.4414	13018.5862	856.0053	62.3223
17153-S_4145	15	1848.1089	1003.5449	3309.4673	3366.518	17672.7383	1304.7101	93.7928
17153-R_back_4134	16	2125.7159	1607.6203	3084.6177	3138.0171	21247.0155	1564.2316	226.5833
17153-R_0438	17	2058.3697	1478.1513	2507.7018	3077.0878	15982.901	1231.4735	321.6037
17153-Q_back_3126	18	1330.635	1429.5197	2563.304	2837.667	16604.9707	882.4041	20.4592
17153-Q_4852	19	1109.1916	1396.8336	2070.6263	2655.4406	16773.6308	451.2039	85.1672



Journal of Nuclear Physics, Material Sciences, Radiation and Applications

Chitkara University, Saraswati Kendra, SCO 160-161, Sector 9-C,
Chandigarh, 160009, India

Volume 7, Issue 2

February 2020

ISSN 2321-8649

Copyright: [© 2020 M. Castro-Colin et al.] This is an Open Access article published in Journal of Nuclear Physics, Material Sciences, Radiation and Applications (J. Nucl. Phy. Mat. Sci. Rad. A.) by Chitkara University Publications. It is published with a Creative Commons Attribution- CC-BY 4.0 International License. This license permits unrestricted use, distribution, and reproduction in any medium, provided the original author and source are credited.